Crystallization of a Weakly Segregated Polyolefin Diblock Copolymer

Pratima Rangarajan[†] and Richard A. Register*

Department of Chemical Engineering, Princeton University, Princeton, New Jersey 08544

Lewis J. Fetters

Exxon Research and Engineering Company, Annandale, New Jersey 08801

Wim Bras[‡]

Netherlands Organisation for Scientific Research and DRAL Daresbury Laboratory, Warrington WA4 4AD, United Kingdom

Steven Naylor and Anthony J. Ryan[§]

Manchester Materials Science Centre, University of Manchester Institute of Science and Technology, Manchester M1 7HS, United Kingdom

Received February 17, 1994; Revised Manuscript Received April 25, 1995[⊗]

ABSTRACT: Microphase separation and subsequent crystallization are studied in an ethylene/head-to-head propylene (E/hhP) diblock copolymer using time-resolved small- and wide-angle X-ray scattering (SAXS and WAXS). When the sample is cooled from the melt, the SAXS data show a broad maximum due to correlation-hole scattering, which is replaced by a single sharp Bragg reflection due to the melt microstructure. During subsequent crystallization, two higher-order reflections grow concurrently. Thus, for similar quench depths below the microphase separation transition (T_{MST}) and the melting temperature (T_m) respectively, microstructures representative of weak and strong segregation are observed. The second- and third-order reflections are superimposed on an intense broad maximum arising from the heterogeneity within the semicrystalline E domains. The second- and third-order SAXS peaks and the broad maximum on which they are superimposed, none of which are visible prior to crystallization, grow in parallel with the development of crystallinity at the unit cell level observed by WAXS. The overall domain periodicity d increases during crystallization but its value is path dependent and varies with the cooling rate from the melt.

I. Introduction

Microphase separation in semicrystalline block copolymers can be driven by block incompatibility or by the crystallization of one or more blocks. Prior work has demonstrated that when the block incompatibility is small, crystallization occurs from a single-phase melt; alternating lamellar microdomains result regardless of the copolymer composition,[1] as anticipated in theoretical treatments.[2,3] A recent time-resolved study[4] using simultaneous small- and wide-angle X-ray scattering (SAXS and WAXS) reported on the development of microstructure from the homogeneous melt in diblocks containing a crystallizable ethylene (E) block. As in homopolymer crystallization, the density differential and sharp interface representative of strong segregation are established as soon as the E block crystallizes. Thus first- and higher-order peaks appear concurrently and develop at the same pace; the development of microstructure also tracks the crystallization of the E block. Similar to microphase-separating amorphous block copolymers, the lamellar domain period and size distribution are invariant during microstructure development. This suggests that the ordered structures nucleate and grow to fill the sample, with no concurrent internal rearrangement. There is, however, a small decrease in domain spacing at longer times which was attributed to the relaxation of amorphous chains which are initially in a nonequilibrium conformation due to the rapid crystallization of the E block.

An added complexity in the case of semicrystalline block copolymers which have large block incompatibilities is the possible formation of an ordered melt mesophase; the presence of these microdomains may affect the crystallization process and the resultant morphology.[5−8] A time-resolved SAXS study of a caprolactone−butadiene (C/B) diblock[5] clearly showed the replacement of the melt microstructure by a crystallization-driven morphology. For this diblock the energy barrier for destruction of the melt morphology was small because of the proximity of the crystallization temperature to the microphase separation temperature (T_{MST}); the diblock is only weakly segregated at the time of crystallization. Moreover, the extremely low molecular weight of the C/B sample provided high chain mobility. Khandpur *et al.*[6] have recently used transmission electron microscopy (TEM) to study the microphase-separated melt structure of polymers with crystallizable E blocks; images of the frozen melt microstructure show severe distortions when the samples are cooled slowly (ice water bath) whereas the melt morphology is preserved if the sample is quenched in liquid nitrogen. Thus, the final morphology of block copolymers crystallizing from two-phase melts depends on several factors which have yet to be explored in detail.

This work employs time-resolved, simultaneous SAXS and WAXS during heating and cooling to study the

* To whom correspondence should be addressed.
[†] Present address: Exxon Chemical Company, P.O. Box 536, Linden, New Jersey 07036.
[‡] Present address: AMOLF, Kruislaan 407, Amsterdam, The Netherlands.
[§] Also DRAL Daresbury Laboratory.
[⊗] Abstract published in *Advance ACS Abstracts,* June 1, 1995.

0024-9297/95/2228-4932$09.00/0

Table 1. Isothermal Crystallization Results

run	$T_m - T_c$ (°C)	initial q^* (nm^{-1})	final q^* (nm^{-1})	$t_{1/2}$ (s) (2nd peak)	initial w_c (30 °C)	final w_c (98 °C)
1	12	0.110	0.137	162	0.37	0.19
2	12	0.136	0.149	188	0.38	0.21

microphase separation and subsequent crystallization of an ethylene/head-to-head propylene, diblock copolymer, denoted E/hhP. As shown below, T_{MST} exceeds the melting point of the crystallized E block, so microphase separation precedes crystallization on cooling from the melt. Comparison of the results with our earlier work[4] on E-based polymers crystallizing from single-phase melts allows some inferences to be drawn regarding the effect of the melt mesophase on crystallization.

II. Experimental Section

A. Synthesis and Characterization. The precursor to the E/hhP is a [high 1,4-polybutadiene]-*block*-[high 1,4-poly(2,3-dimethyl-1,3-butadiene)] which was synthesized by sequential anionic polymerization in cyclohexane.[9] The E/hhP diblock is obtained after exhaustive hydrogenation of the precursor in heptane solution at 80–100 °C and 300 psi hydrogen using palladium on barium sulfate as catalyst.[10] Sample E52 is a hydrogenated polybutadiene homopolymer (M_w = 52 kg/mol) of similar microstructure to the E block in the E/hhP diblock; it has been characterized previously.[4] ^{1}H nuclear magnetic resonance (NMR) on the precursor diblock was used to determine the weight fraction of E block in the copolymer (f, ± 3% relative) and the microstructure of the precursor 1,4-polybutadiene (6% 1,2) and poly(dimethylbutadiene) (2.5% 1,2) blocks. The total molecular weight of the precursor diblock was estimated using this value of f (0.51) and the molecular weight of the 1,4-polybutadiene block which was determined by size exclusion chromatography (SEC). The molecular weight (M_w) of the E/hhP was calculated to be 50.3 kg/mol with a polydispersity of 1.04 (SEC of precursor diblock). Fourier transform infrared (FTIR) spectroscopy and ^{13}C-NMR were used to verify that there was no residual unsaturation in the diblock after hydrogenation. The peak melting temperature (T_m, 110 °C) of the material was determined at a scan rate of 20 °C/min, using a Perkin-Elmer DSC-7 calibrated with indium and mercury. Static SAXS data were collected at different temperatures using a compact Kratky camera with a hot stage and a Braun position-sensitive detector. The data were reduced using previously reported procedures[11] to background-subtracted, desmeared absolute intensity versus the scattering vector $q = (4\pi/\lambda) \sin \theta$, where λ is the radiation wavelength and 2θ the scattering angle. The total lamellar repeat distance (d), which is the sum of the E and hhP domain widths, is determined from the position of the first peak q^* in the q^2-corrected[12] data:

$$d = 2\pi/q^* \tag{1}$$

All SAXS data presented here have had the intensities multiplied by q^2 in anticipation of an alternating lamellar microstructure.

B. Time-Resolved Experiments. Time-resolved simultaneous SAXS/WAXS experiments were conducted at beamline 8.2 of the Synchrotron Radiation Source in Daresbury.[4,13] A 2 mm thick film of the polymer sample was enclosed in a cell made of standard aluminum differential scanning calorimetry (DSC) pans (TA Instruments) with holes punched in both the pan and the lid and covered with 25 μm thick mica windows. A 1.0 × 2.5 mm^2 slot in the heater block and cell holder, a modified Linkam THM microscope hot stage with a high resolution dc temperature controller, allows X-rays access to the sample.[14] Cooling of the sample cell is achieved via cold nitrogen vapor pumped through the heater block. Equilibrium values of the cell temperature were verified by comparison of crystallization half-times with those obtained from isothermal crystallization on other block copolymers[4] conducted on a Perkin-Elmer DSC-7. Due to thermal lag between the sample and the sensor thermocouple (outside the sample cell) during heating or cooling, the quoted temperatures during these ramps are nominal values only. The SAXS data are collected with a Daresbury quadrant detector for which angular calibration was done with a rattail tendon. The SAXS data presented here were subsequently smoothed with a five-point triangle function and an additional nine-point triangle for $q > 0.2$ nm^{-1}. Except where noted (Figure 4), SAXS peak intensities were determined by summing five channels around the peak. The WAXS data were acquired with a curved INEL detector which was cross-calibrated with data collected in reflection mode on a Philips-Norelco wide-range goniometer using Cu Kα radiation. Subsequent smoothing of the WAXS data employed a five-point triangle function and an additional eleven-point triangle for the data outside the crystalline peaks. The areas under the crystallite reflections (I_c) and the amorphous hump (I_a) in the WAXS data can be used to estimate the weight fraction crystallinity (w_c) within the E block:

$$w_c = \frac{1}{f}\left(\frac{I_c}{I_c + I_a}\right) \tag{2}$$

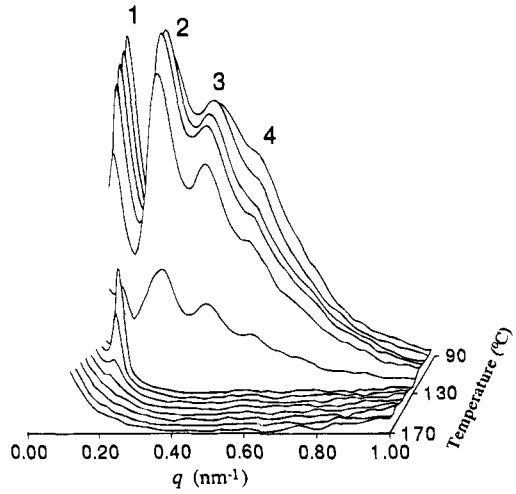

Figure 1. SAXS data for the E/hhP diblock on heating during run 2. Vertical axis is q^2-corrected intensity (linear scale); nominal values of sample temperature are given on the depth axis, with time increasing from back to front. Each curve is the intensity integrated over 18 s. Numbers 1–4 indicate the reflection order from an alternating lamellar microstructure.

Table 1 lists the initial and final values for w_c for both runs.

Prior to run 1, the diblock was heated to 135 °C and allowed to flow under its own weight into a 2 mm thick film which was slow cooled (20 °C/min) and annealed at 76 °C for 24 h. The temperature profile for the time-resolved experiments was as follows. *Run 1*: 1 min hold at 30 °C, followed by 20 °C/min ramp up to the melt temperature (T_{melt}) of 148 °C, 2 min hold at T_{melt}, followed by ~20 °C/min cool-down to the crystallization temperature (T_c) of 98 °C. *Run 2*: 1 min hold at 30 °C, followed by 20 °C/min ramp up to 198 °C (T_{melt}), followed by ~30 °C/min cool-down to 98 °C (T_c). Data acquisition commenced after the 1 min hold at 30 °C; each frame consists of the intensity integrated over a 6 s period. Because the primary SAXS peak was hidden by the beamstop during run 1, the sample to detector distance was increased prior to run 2 in order to access lower angles.

III. Results and Discussion

Figure 1 is a plot of the q^2-corrected SAXS data as the sample heats to 170 °C during run 2; for clarity, every three data sets have been averaged so that each curve represents the intensity averaged over an 18 s period. The primary peak position (q^*) at the beginning of run 2 is 0.136 nm^{-1}. At 90 °C, four reflections are evident at q/q^* of 1:2:3:4, as is expected from a well-

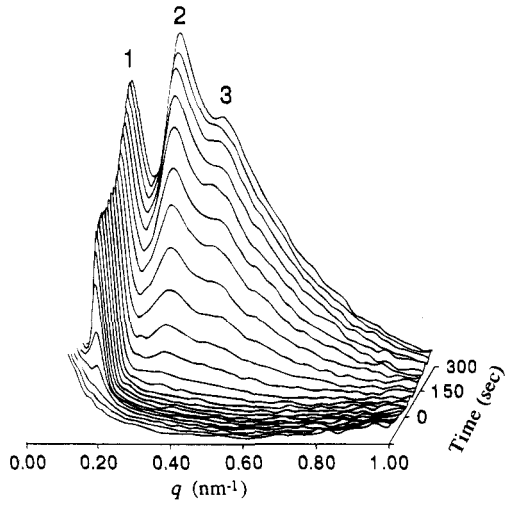

Figure 2. SAXS data for the E/hhP diblock during isothermal crystallization at 98 °C. Time = 0 corresponds to the time at which the DSC thermocouple first registers T_c (98 °C). The peak apparent in the data for time < 0 is representative of the melt microstructure.

ordered lamellar sample, and they all disappear by 124 °C. This disappearance can be attributed to the melting of the E crystallites, which have a final T_m of 115 °C. These SAXS patterns are unusual in that the second-, third-, and fourth-order peaks are quite strong relative to the primary peak prior to the melting of the E crystallites. This unexpected result stems from the strong scattering from within the heterogeneous E domain, which contains both crystalline and amorphous E. This effect is discussed in detail below, following the discussion of the changes which occur in the first-order SAXS peak during both microphase separation and crystallization.

After the E crystallites have fully melted, a much sharper peak appears at $q^* = 0.165$ nm^{-1}. With continued heating, this narrow peak broadens and declines in intensity, as would be expected for a diblock heated above its microphase separation transition (MST). The MST temperature for the E/hhP diblock, T_{MST}, can be estimated from the temperature-dependent Flory interaction parameter, $\chi(T)$, between E and hhP. The E/hhP diblock has an E block weight fraction (f) of 0.51, so following mean-field theory,[15] the MST should occur at $(\chi N_n)_{MST} \approx 10.5$. The number-average degree of polymerization N_n of the diblock, choosing a segment molecular weight of 56 g/mol for both blocks,[15] is 864. Using data obtained from small-angle neutron scattering on polyolefin blends and the solubility parameter formalism developed by Graessley and co-workers,[16,17] for a segment molecular weight of 56 g/mol the $\chi(T)$ relation for E/hhP is

$$\chi \times 10^3 = -14.1 + 11200/T \qquad (3)$$

For $\chi_{MST} = 10.5/864$, this equation yields $T_{MST} \approx 154$ °C, so our diblock is expected to be microphase separated in the melt; the single sharp peak at $q^* = 0.165$ nm^{-1} can therefore be attributed to the melt microstructure.

The reverse of this process occurs while cooling the sample from 198 °C to T_c. Figure 2 shows SAXS data for the E/hhP diblock during isothermal crystallization at 98 °C; since $t = 0$ is the time at which the DSC thermocouple first registers T_c, data sets prior to $t = 0$ are not temperature invariant but represent various stages of the cooling ramp. At about 122 °C ($t = -60$ s

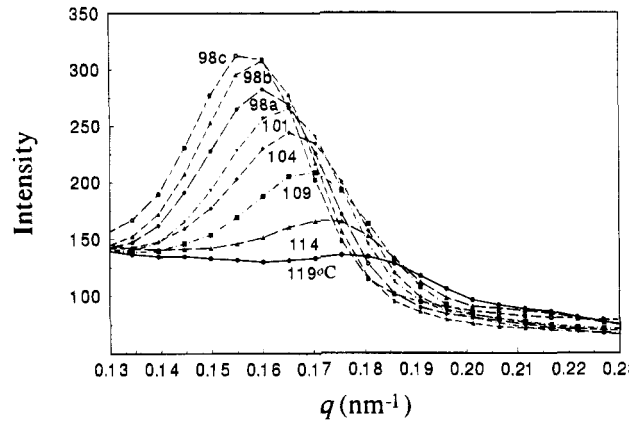

Figure 3. Expanded view of the development of the melt microstructure in the E/hhP diblock. Temperatures greater than 98 °C are nominal values only. The peaks marked 98 °C represent the time evolution of the structure at constant temperature: (a) 0 s; (b) 30 s; (c) 90 s.

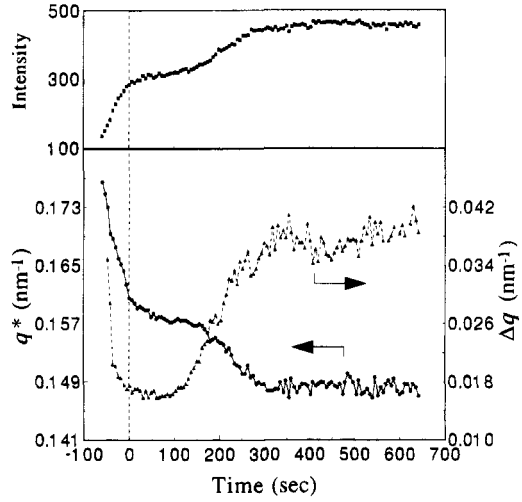

Figure 4. Peak position q^* (●, left axis), peak width Δq (▲, right axis), and peak intensity (■, top) vs time for the first-order peak in the SAXS data for the E/hhP diblock. The dashed line represents the time at which the thermocouple reaches T_c.

in Figure 2) a broad peak appears and grows in intensity until the sample reaches T_c ($t = 0$). From the expanded view of this peak shown in Figure 3, it is obvious that the peak shape also changes dramatically during this time; although the initial broad peak is reminiscent of disordered-state correlation-hole scattering, when T_c (98 °C) is reached, the peak is quite sharp as expected from a Bragg reflection of a microphase separated material.[18,19]

Previous equilibrium scattering studies of block copolymers near the MST have found that although q^* varies continuously,[18-20] the peak width Δq shows a definite discontinuity at the transition[18,20] and assumes a relatively constant value for $T < T_{MST}$. Figure 4 is a plot of q^*, peak width (Δq), and peak intensity versus time for the first-order SAXS reflection; here the intensity is determined at the peak maximum, and Δq is the full width at 85% of maximum intensity. There is a 50% decrease in Δq on cooling prior to crystallization (Figure 4, $-60 < t < 0$ s) and a 9% reduction in q^*. Closer examination of the data for $t < 0$ in Figure 4 reveals a steep change in peak intensity, Δq, and q^* between 109 °C (−36 s) and 112 °C (−42 s), although all three parameters continue to change before and after this point. On heating, similar changes in these pa-

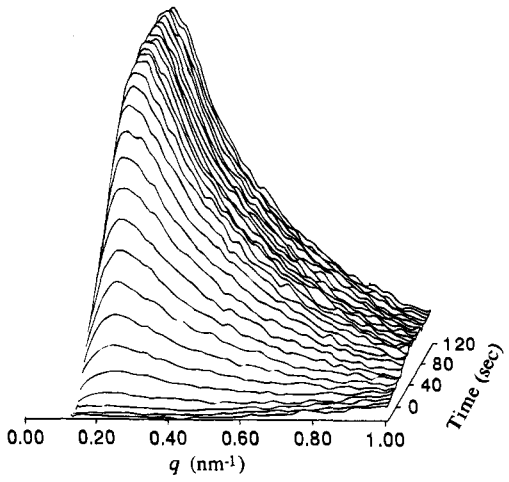

Figure 5. SAXS data for the hydrogenated polybutadiene E52 during cooling. Time = 0 corresponds to the time at which the DSC thermocouple first registers T_c (88 °C). E52 crystallizes rapidly, and detectable crystallization occurred beginning about 30 s prior to reaching T_c.

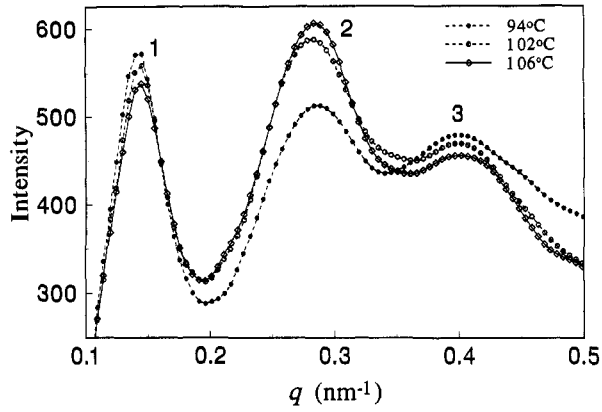

Figure 6. SAXS data showing changes in relative peak intensity during the heating ramp. The nominal values of temperature corresponding to each data set are 94 (●), 102 (○), and 106 °C (◇). Numbers 1–3 indicate the reflection order from an alternating lamellar microstructure.

rameters were observed around 132 °C. The difference between the apparent T_{MST} on heating (132 °C) and cooling (110 °C) arises from two factors, thermal lag and microphase separation kinetics. Because the sample is heated or cooled rapidly (20–30 °C/min), the actual temperature of the sample tends to lag behind the nominal temperature, which is measured outside the sample pan; moreover, a thermal gradient will be present across the sample. This produces an apparent heating–cooling hysteresis, as well as broadening any thermal transitions. In addition, the material requires a finite amount of time to order[21,22] once quenched below T_{MST}. Since our experimental protocol cools the sample continuously, any time required for the ordering will tend to depress the observed value of T_{MST}. Considering these two effects, a reasonable assignment for our sample is $T_{MST} \simeq 125$ °C, which compares adequately with the calculated value of 154 °C. The value of 125 °C is also consistent with the observation that the E/hhP sample flows under its own weight[1,23] at 135 °C.

With increasing time at 98 °C, two higher-order peaks appear in the SAXS data (Figure 2), which are similar to the unusual pattern observed during heating (Figure 1) in that the second- and third-order peaks are of comparable intensity to the first-order reflection. This unusual situation occurs because the SAXS patterns in the crystallized diblock actually contain contributions both from the overall domain structure (alternating E and hhP layers; in Figure 2, $q^* = 0.148$ nm^{-1}, so $d =$ 42.5 nm) and from the internal structure of the E domains (alternating E crystallites and amorphous E regions, $d \approx 21$ nm). Figure 5 shows SAXS data for the hydrogenated polybutadiene E52, the "homopolymer" analog of the E block, crystallizing at a nominal temperature of 88 °C. E52 exhibits a single broad peak with its maximum at 0.3 nm^{-1} (denoted $q^\dagger$), but with substantial intensity extending out to nearly 1.0 nm^{-1}. Comparison of Figures 2 and 5 reveals that the SAXS data at higher q (above 0.2 nm^{-1}) for the E/hhP diblock consist of an intense broad component very similar to the SAXS pattern of E52 and weaker narrow components corresponding to the second and third orders of the principal reflection at $q^* = 0.148$ nm^{-1}. We have previously reported[1] similar superposition of two SAXS patterns in ethylene–(ethylene-*alt*-propylene) diblocks (E/EP), with periodicities corresponding to q^* and $q^\dagger$, but the scattering was dominated by the peaks at multiples of q^*. In the present E/hhP case, the smaller electron density difference between the E and hhP domains (compared with E *vs* EP) reduces the intensity of the reflections arising from alternating E and hhP layers, which are the narrow components at q^*, $2q^*$, and $3q^*$. The broad maximum centered at $q^\dagger$ (corresponding to the scattering between amorphous and crystalline E) is of the same intensity in the E/hhP and E/EP systems, and thus the two types of scattering appear with similar intensity in the E/hhP diblock.

This weak electron density contrast between E and hhP domains decreases further with increasing temperature as the E crystallites melt. From the known densities and thermal expansion coefficients,[15,17,24,25] the density of hhP is calculated to lie between the densities of amorphous and crystalline E. Thus, as the weight fraction crystallinity in the E block (w_c) is reduced, the overall electron densities of E and hhP approach each other; for a temperature of 98 °C, they are calculated to cross when $w_c = 0.12$. In fact, there is a brief period prior to melting when the first-order peak in the E/hhP diblock decreases in intensity while the second-order peak appears to grow (Figure 1, expanded view in Figure 6). The apparent increase in the intensity of the second-order peak arises from changes in the broad maximum on which it rides. Because the E block and the E52 sample can be thought of as random copolymers of ethylene with a minor amount of 1-butene, they form a wide distribution of crystallite sizes which melt over a range of temperatures. As the sample is heated and the thin crystallites melt, the remaining crystallites are spaced further apart and the broad SAXS maximum moves to lower q. At room temperature,[1] $q^\dagger \approx 0.5$ nm^{-1} for E52, while at 88 °C, $q^\dagger \approx 0.3$ nm^{-1}. Additional data[26] for E52 show a smooth movement of the broad maximum to lower q as temperature is increased.

With this understanding of the morphological origin of the SAXS patterns, we can proceed to analyze the kinetics of structure development. Since the E/hhP diblock is weakly segregated in the melt, it shows no higher-order reflections until it begins to crystallize (Figure 2). Both the narrow ($2q^*$, $3q^*$) and broad ($q^\dagger$) components of the scattering at $q > 0.2$ nm^{-1} arise from crystallization, so the time evolution of intensity at q values corresponding to the higher orders reflects crystallization only, with no contribution from melt microphase separation. This time evolution can be

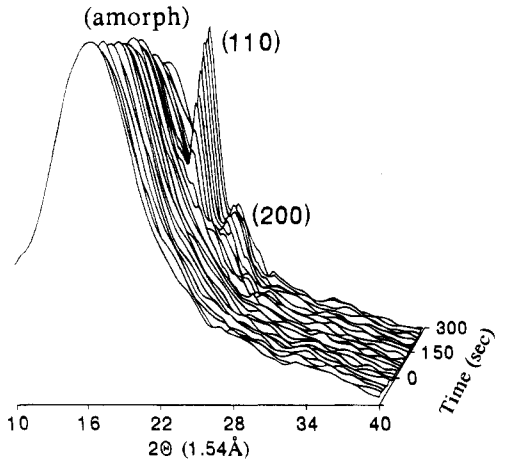

Figure 7. WAXS data corresponding to the SAXS data in Figure 2. Peaks labeled (110) and (200) are the reflections of the orthorhombic polyethylene unit cell; (amorph) represents the scattering from the hhP and amorphous E.

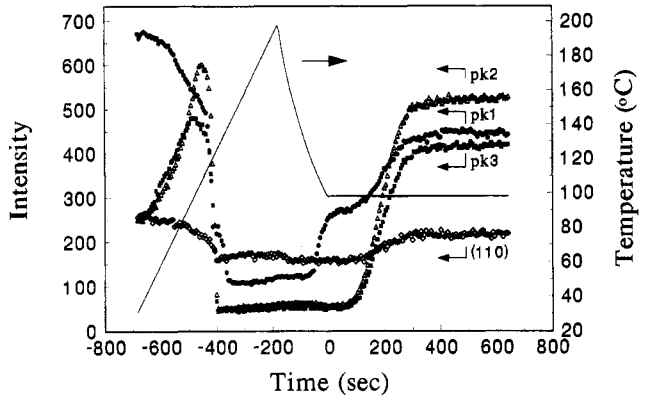

Figure 8. Peak intensity vs time for the first three SAXS reflections and WAXS (110) peak (◇). Final SAXS peak positions are (●) $q_1 = 0.149$ nm^{-1}, (△) $q_2 = 0.295$ nm^{-1}, and (■) $q_3 = 0.447$ nm^{-1}. Time = 0 is the time at which the DSC thermocouple first registers T_c. The solid line represents the temperature, which is referenced to the right axis.

compared with that seen at the unit cell level by WAXS. Figure 7 shows the WAXS frames which correspond to the SAXS data for $t > 0$ in Figure 2; the large amorphous hump characteristic of the melt scattering at $t = 0$ decreases in intensity as the (110) and the (200) crystallite reflections of the orthorhombic PE crystal[24] grow in, beginning around 100 s. The intensities of the first three SAXS reflections, as well as the WAXS (110) reflection, are shown for the entire heating, cooling, and isothermal crystallization cycle in Figure 8. The first-order SAXS peak emerges at the MST (−70 s in Figure 8) and remains nearly unchanged for $0 < t < 80$ s, after which it undergoes another increase in intensity concurrent with the growth of the two higher-order peaks and the growth of the WAXS (110) reflection. As discussed in our previous publication,[4] it is easiest to compare the growth rates on an Avrami plot. The Avrami equation is

$$\ln(1 - X_c) = -kt^n \tag{4}$$

In polymer crystallization under nonflow conditions, X_c is generally taken as the volume fraction of material that is filled with spherulites, k and n are adjustable parameters, and t is the time elapsed. Time-resolved small-angle light scattering measurements[27] show that the E/hhP diblock gives the four-leaf-clover H_v pattern

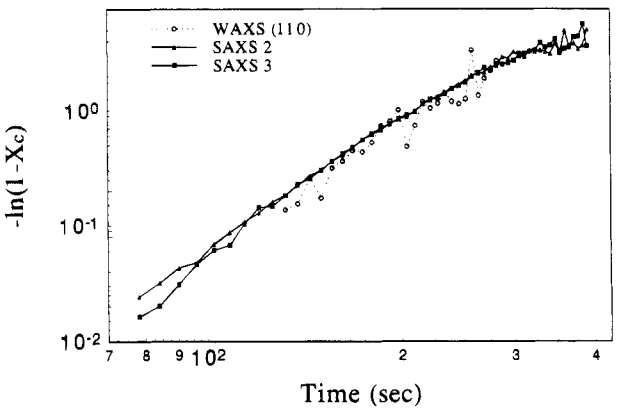

Figure 9. Avrami plot of the second- (▲) and third-order (■) SAXS peaks and the (110) WAXS (○) reflection for the E/hhP sample during crystallization at 98 °C.

characteristic of spherulites for conditions ranging from a slow cool (2 °C/min) to a quench in ice water, although the pattern is poorly developed in comparison with that exhibited by ethylene−(ethylene-*alt*-propylene) diblocks (E/EP).[1,27] Optical microscopy also confirms the existence of spherulites in the E/hhP sample, although they do not appear as symmetric and well developed as those formed by a hydrogenated polybutadiene homopolymer or an E/EP diblock crystallized from a single-phase melt.[28] We have determined X_c from the SAXS and WAXS data using the following expression:

$$X_c = \frac{I(t) - I_0}{I_m - I_0} \tag{5}$$

where I_0 is the melt scattering intensity at T_c (determined from the data set at $t = 0$), I_m is the intensity at the end of the experiment, and $I(t)$ is the intensity at time t. Figure 9 shows that the two higher-order SAXS peaks and the WAXS (110) peak track each other during the formation of the crystalline microstructure, similar to our prior results for diblocks which crystallize from single-phase melts.[4] The crystallization half-times ($t_{1/2}$; $t = t_{1/2}$ when $X_c = 0.5$) for the two runs are listed in Table 1. The parallel growth of SAXS and WAXS data confirms that this stage of domain structure development is driven by crystallization of the E block.

During crystallization ($80 < t < 300$ s) there is also continuous movement of the first-order peak to lower angle, after which it assumes a constant position indicative of no further restructuring (Figure 4). In the C/B diblock studied by Nojima *et al.*,[5] crystallization results in a distinct peak at much lower q which grows at the expense of the melt peak; the half-time for the crystalline peak coincides with the time at which the melt peak has declined to half its maximum intensity. In our E/hhP diblock, the crystalline reflection also grows in at the expense of the melt peak; at any point in the growth process the peak shape can be approximated by a linear combination of the melt scattering at $t = 0$ and the crystalline peak at the end of the run, with the weights corresponding to $1 - X_c$ and X_c, respectively. Thus, the absence of a distinct peak is simply due to the small change in peak position relative to the C/B case. The first-order SAXS peak is also substantially broader after crystallization than in the melt (130% increase in Δq, Figure 4), indicating a much wider domain size distribution. As discussed in our prior publications,[1,4] the semicrystalline block copolymer morphology consists of relatively irregular E

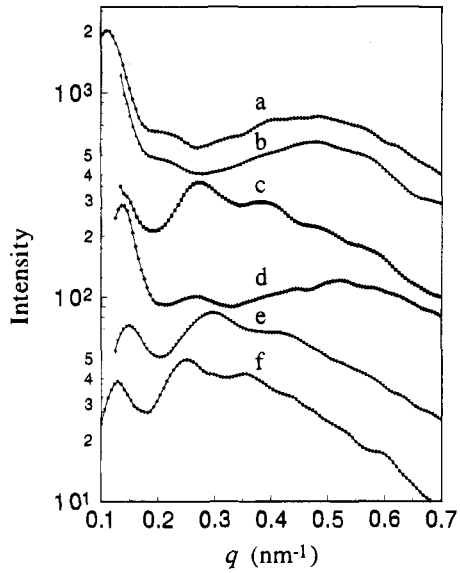

Figure 10. Comparison of E/hhP SAXS data for different thermal histories. The vertical (logarithmic) axis is the q^2-corrected intensity plotted on an arbitrary scale. (a) Kratky data at 25 °C, sample previously annealed at 76 °C; (b) synchrotron data at 30 °C, first frame of run 1; (c) synchrotron data at 98 °C, last frame of run 1; (d) synchrotron data at 30 °C, first frame of run 2; (e) synchrotron data at 98 °C, last frame of run 2; (f) Kratky data at 98 °C.

domains interspersed with amorphous domains of uniform thickness; thus greater domain irregularity is introduced when the E block crystallizes.

The positions of the first-order reflection in the E/hhP diblock obtained at the beginning ($q^* = 0.136$ nm^{-1}) and the end of run 2 (0.149 nm^{-1}) differ considerably, implying that the final morphology of this E/hhP sample is *path dependent*. Therefore, the effect of different thermal treatments on the domain periodicity was examined in some detail. Figure 10 shows SAXS patterns for the E/hhP diblock taken at both room temperature and 98 °C after several thermal histories. Patterns acquired at room temperature (Figure 10a,b,d) show a broad scattering maximum centered around 0.5 nm^{-1}, due to the heterogeneity within the E domain; at elevated temperatures, this broad maximum moves to 0.3 nm^{-1}, as discussed above. The starting E/hhP specimen, which had been crystallized during slow cooling and annealed as described in section IIB, shows $q^* = 0.110$ nm^{-1}, or $d = 57$ nm (Figure 10a, Kratky camera data). At the end of run 1, after isothermal crystallization at 98 °C, the second- and third-order reflections are quite strong (Figure 10c); from the positions of these peaks q^* is calculated to be 0.137 nm^{-1} ($d = 46$ nm). This value of q^* is roughly reproduced (0.136 nm^{-1}) in the first data set of run 2 (Figure 10d, at 30 °C), indicating that minimal domain-structure rearrangement occurred during the 24 h between runs. At the end of run 2, after another isothermal crystallization cycle at 98 °C (Figure 10e), $q^* = 0.149$ nm^{-1} ($d = 42$ nm). The initial and final values of q^* are listed in Table 1; for comparison, recall that in the melt $q^* = 0.165$ nm^{-1}.

These substantial changes in q^* indicate that the domain periodicity is sensitive to even minor changes in thermal history; runs 1 and 2 differ primarily in their cooling rate from the melt. Since no path dependence was seen in our E/EP samples,[4] this sensitivity can only be attributed to the melt segregation in the E/hhP. In order to investigate this path dependence further,

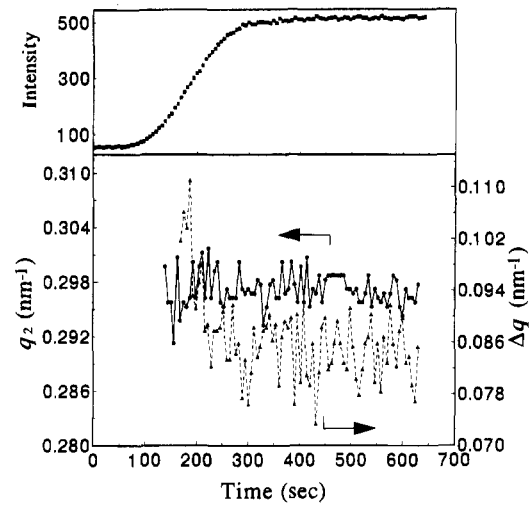

Figure 11. Peak position (●, left axis), peak width (▲, right axis), and peak intensity (■, top) vs time for the composite second-order SAXS peak (at $q_2 \approx 2q^* \approx q^\dagger$), which contains contributions from the E/hhP domain structure as well as from the heterogeneity within the E domains.

equilibrium SAXS data were acquired using the Kratky setup after cooling from 160 to 99 °C (±3 °C) at a rate of 2−3 °C/min; the data show two peaks, at 0.128 and 0.256 nm^{-1}, corresponding to $d = 49$ nm (Figure 10f).

A value of d can also be calculated from a scaling relationship for d as a function of block copolymer composition and molecular weight.[1] The experimentally determined relationship using E/EP diblocks crystallized from single-phase melts can be considered to represent the equilibrium crystallization-driven scaling for that system. Since the E/EP and E/hhP systems are somewhat different and since the scaling law is only an approximate description of the E/EP behavior, this relationship can provide a rough estimate only; the calculated $d = 63$ nm is closest to the experimental value (57 nm) for the starting E/hhP sample, which had been slow-cooled and annealed. Evidently, the slower cooling rates facilitate the large-scale structural reorganization needed to change the morphology from that established in the melt, where $d = 38$ nm.

For the E/hhP diblock, after ~300 s there is no further change in SAXS intensity, peak position, or peak width (Figures 4 and 11) or the WAXS crystallinity (Figure 8). In contrast, the E/EP diblocks which crystallized from single-phase melts showed a secondary slow but definite increase in the SAXS and WAXS intensity and in q^* during this stage.[4] The increase in intensity was attributed to the creation of new lamellar stacks and the increase in q^* to the contraction of the EP domain from a nonequilibrium conformation frozen in during crystallization. Since the E/hhP morphology is path dependent, the absence of restructuring is not because the diblock has reached equilibrium, but may be due to the additional hindrance to structural rearrangement imposed by the larger value of χN.

For diblocks crystallizing from homogeneous melts, we have previously[1] proposed a morphology wherein the E crystallites run parallel to the domain interfaces. For diblocks crystallizing from two-phase melts of moderate to high segregation strength, Douzinas and Cohen[29] used pole-figure analysis on oriented samples to show that the opposite occurs, *i.e.*, the E crystallites run perpendicular to the domain interfaces. Since the E/hhP diblock studied here lies between the two extremes, it is appropriate to ask which case pertains, if

either. Because our samples are unoriented, we cannot directly determine the direction of chain folding, but the formation of spherulites from the quiescent melt suggests that the E/hhP diblock resembles the E/EP diblocks crystallizing from single-phase melts. In addition, inserting a full-wave (530 nm) plate between the polarizers in optical microscopy[28,30] colors two quadrants of each spherulite orange and two quadrants blue, indicating the orientation of the fast axis in each quadrant. A hydrogenated polybutadiene homopolymer, an E/EP diblock crystallized from a single-phase melt, and the E/hhP diblock all show the same orange/blue quadrant pattern, indicating that the chain axis is oriented tangentially in all three cases.

IV. Conclusions

Structure formation in a crystallizable E/hhP diblock was investigated using static and time-resolved SAXS and WAXS on heating and cooling. T_{MST} for this diblock is approximately 125 °C; since all the E crystallites melt by 115 °C, crystallization occurs from the weakly segregated melt. Only a single SAXS peak is present in the melt, but after crystallization the sample shows 3–4 SAXS peaks, typical of a strongly segregated material. The higher-order reflections in the SAXS data are superimposed on an intense broad maximum arising from scattering contributed by the heterogeneity within the E domains (alternation of E crystallites and amorphous E), causing the higher-order peaks to appear quite intense. During isothermal crystallization, the higher-order SAXS reflections and the WAXS peaks grow concurrently, indicating that the alteration in microdomain structure induced by crystallization occurs simultaneously with the development of crystallinity.

During crystallization, the first-order SAXS peak moves continuously to lower angle with a concurrent increase in peak width. The peak shape and position during crystallization can be adequately approximated by a linear combination of the peaks observed before and after crystallization, consistent with a nucleation and growth process where melt is simply converted to crystallized material with no subsequent change in morphology. The position of the first-order SAXS peak after crystallization, which reflects the overall domain periodicity, is sensitive to even minor changes in the sample's thermal history. As the cooling rate from the melt decreases, the change in the domain periodicity between the molten and crystallized diblock increases. Microphase separation evidently presents a substantial barrier to the large-scale structural reorganization which occurs on crystallization; path dependence has not been observed in E/EP diblocks crystallizing from homogeneous melts. Also in contrast to E/EP diblocks, after the primary crystallization process the E/hhP diblock shows no further change in domain spacing. Since the sample has not reached its equilibrium domain spacing, the unchanging value must reflect additional barriers to rearrangement in the crystallized material imposed by the segregation between E and hhP blocks.

Acknowledgment. Support for this research (to P.R. and R.A.R.) was provided through the National Science Foundation, Polymers Program (Grant DMR-9257565) and the NEC Preceptorship at Princeton University. P.R. would like to thank C. B. Gell of Princeton for invaluable help with sample preparation, and D. J. Quiram of Princeton for development of the Kratky camera hot stage. Finally, P.R. and R.A.R. wish to thank H. E. King, Jr., of Exxon Research and Engineering Co. for providing expertise and equipment essential for the optical microscopy measurements.

References and Notes

(1) Rangarajan, P.; Register, R. A.; Fetters, L. J. *Macromolecules* **1993**, *26*, 4640.
(2) Di Marzio, E. A.; Guttman, C. M.; Hoffman, J. D. *Macromolecules* **1980**, *13*, 1194.
(3) Whitmore, M. D.; Noolandi, J. *Macromolecules* **1988**, *21*, 1482.
(4) Rangarajan, P.; Register, R. A.; Adamson, D. H.; Fetters, L. J.; Bras, W.; Naylor, S.; Ryan, A. J. *Macromolecules* **1995**, *28*, 1422.
(5) Nojima, S.; Kato, K.; Yamamoto, S.; Ashida, T. *Macromolecules* **1992**, *25*, 2237.
(6) Khandpur, A. K.; Macosko, C. W.; Bates, F. S. *J. Polym. Sci., B: Polym. Phys.* **1995**, *33*, 247.
(7) Cohen, R. E.; Cheng, P. L.; Douzinas, K.; Kofinas, P.; Berney, C. V. *Macromolecules* **1990**, *23*, 324.
(8) Séguéla, R.; Prud'homme, J. *Polymer* **1989**, *30*, 1446.
(9) Morton, M.; Fetters, L. J. *Rubber Chem. Technol.* **1975**, *48*, 359.
(10) Rosedale, J. H.; Bates, F. S. *J. Am. Chem. Soc.* **1988**, *110*, 3542.
(11) Register, R. A.; Bell, T. R. *J. Polym. Sci., B: Polym. Phys.* **1992**, *30*, 569.
(12) Russell, T. P. In *Handbook on Synchrotron Radiation*; Brown, G. S., Moncton, D. E., Eds.; North-Holland: New York, 1991; Vol. 3.
(13) Bras, W.; Derbyshire, G. E.; Ryan, A. J.; Mant, G. R.; Felton, A.; Lewis, R. A.; Hall, C. J.; Greaves, G. N. *Nucl. Instrum. Methods Phys. Res. A* **1993**, *326*, 587.
(14) Bras, W.; Derbyshire, G. E.; Devine, A.; Clark, S. M.; Cooke, J.; Komanschek, B. E.; Ryan, A. J. *J. Appl. Crystallogr.* **1995**, *28*, 26.
(15) Bates, F. S.; Schulz, M. F.; Rosedale, J. H.; Almdal, K. *Macromolecules* **1992**, *25*, 5547.
(16) Graessley, W. W.; Krishnamoorti, R.; Balsara, N. P.; Butera, R. J.; Fetters, L. J.; Lohse, D. J.; Sissano, J. A. *Macromolecules* **1994**, *27*, 3896.
(17) Graessley, W. W.; Krishnamoorti, R.; Reichart, G. C.; Balsara, N. P.; Fetters, L. J.; Lohse, D. J. *Macromolecules* **1995**, *28*, 1260.
(18) Hashimoto, T.; Ogawa, T.; Han, C. D. *J. Phys. Soc. Jpn.* **1994**, *63*, 2206.
(19) Bates, F. S.; Rosedale, J. H.; Fredrickson, G. H. *J. Chem. Phys.* **1990**, *92*, 6255.
(20) Winey, K. I.; Gobran, D. A.; Xu, Z.; Fetters, L. J.; Thomas, E. L. *Macromolecules* **1994**, *27*, 2392.
(21) Floudas, G.; Pakula, T.; Fischer, E. W.; Hadjichristidis, N.; Pispas, S. *Acta Polym.* **1994**, *45*, 176.
(22) Hashimoto, T. *Macromolecules* **1987**, *20*, 465.
(23) Bates, F. S.; Rosedale, J. H.; Bair, H. E.; Russell, T. P. *Macromolecules* **1989**, *22*, 2557.
(24) Howard, P. R.; Crist, B. *J. Polym. Sci., B: Polym. Phys.* **1989**, *27*, 2269.
(25) Brandrup, J.; Immergut, E. H., Eds. *Polymer Handbook*, 3rd ed.; Wiley: New York, 1989; p V/15.
(26) Rangarajan, P. Ph.D. Thesis, Princeton University, 1995.
(27) Ueda, M. M.S.E. Thesis, Princeton University, 1995.
(28) Rangarajan, P.; Fetters, L. J.; King, H. E., Jr.; Quiram, D. J.; Register, R. A., unpublished data.
(29) Douzinas, K. C.; Cohen, R. E. *Macromolecules* **1992**, *25*, 5030.
(30) Hartshorne, N. H.; Stuart, A. *Crystals and the Polarising Microscope*, 4th ed., American Elsevier: New York, 1970.

MA9501555